Robust Metal-Ceramic Coaxial Cable Sensors for Distributed Temperature Monitoring in Fossil Energy Power Systems

Project #: *DE-FE-0022993* **(UCR/NETL/DOE)**
DOE Project Manager: *Jessica Mullen*
Project Term: 36 months (7/1/14 – 6/30/17)

Principal Investigator: Junhang Dong, University of Cincinnati
Subcontractor: Hai Xiao, Clemson University

Student Participants: Adam Trontz and Shixuan Zeng (U. Cin.); Baokai Cheng (Clemson U.)

NETL/U.S. Department of Energy
Cross-Cutting Technology Research Review Meeting, April 18-19, 2016, Pittsburgh, PA

Presentation Outline

- Project Objective
  - New MCCC-FPI sensor
- Project Status
- Background
- MCCC-FPI Sensor
  - Concept and Principle of Sensor Operation
  - Hurdles to developing MCCC-FPI
- Research Focus
  - Material Development; Sensor Fabrication; Sensor Testing
- Conclusions and Plans

1. Project Objectives

Goal of Project: To develop a new type of low cost, robust metal-ceramic coaxial cable (MCCC) Fabry-Perot interferometer (FPI) sensor and demonstrate the capability of cascading a series of FPIs in a single MCCC for real-time distributed monitoring of temperature up to 1000^{o}C.

Specific objectives:

1. Identify MCCC Sensor Materials
   - Dielectric properties; thermochemical, chemical and structural stability; cost
2. MCCC-FPI sensor fabrication
3. Instrumentation for sensor operation and signal processing
4. Demonstration/evaluation of MCCC-FPI sensors
   - Distributed temperature measurement
   - Sensitivity
   - Spatial resolution
   - Stability
   - Response speed

2. Project Status

Phase-I Goal:

Single point MCCC-FPI sensor to achieve temperature measurement up to 500^{o}C at ±2^{o}C resolution/accuracy

Status: Accomplished on time

									Project Year 3 (7/1/16-6/30/17)					Planned end date
									Q8	Q9	Q10	Q11	Q12	
														7/31/14
														12/31/14
														6/30/15
														12/31/15
														6/30/15
4.1	1. Design cascaded MCCC-FPI sensors and develop instrumentation and algorithms for distributed sensing					•	•	•						12/31/16
4.2	2. Fabrication of the multiple-point MCCC-FPI sensor (2 -3 FPI)							•	•	•				12/31/16
5.0	1. Fabricated Multipoint FPIs (16 Pts) in ~2m-long MCCC.									•	•	•	•	6/30/17
	2. Demonstrated 16 FPIs in ~2m-long MCCC for distributed temperature measurement up to 1000^{o}C with spatial resolution <10cm.											•	•	6/30/17

3. Background

- Advanced power generation from coal
  - Ultra Supercritical (USC) steam cycle design (760 ^{o}C)
  - Oxy-Fuel firing and Integrated Gasification Combined Cycle (~1000 ^{o}C)
- Need for sensing and monitoring
  - Process Conditions
  - Equipment Physical States

4. Coaxial Cable vs Optical Fiber —EM Wave Transmission

- Both for EM transmission/communication
- Same governing theory (physics)
- Different frequency ranges of carried EM
- Coaxial cable is more robust than optical fiber
- Both waveguides are useful for constructing sensors
- Readiness for instrumentation for sensor system

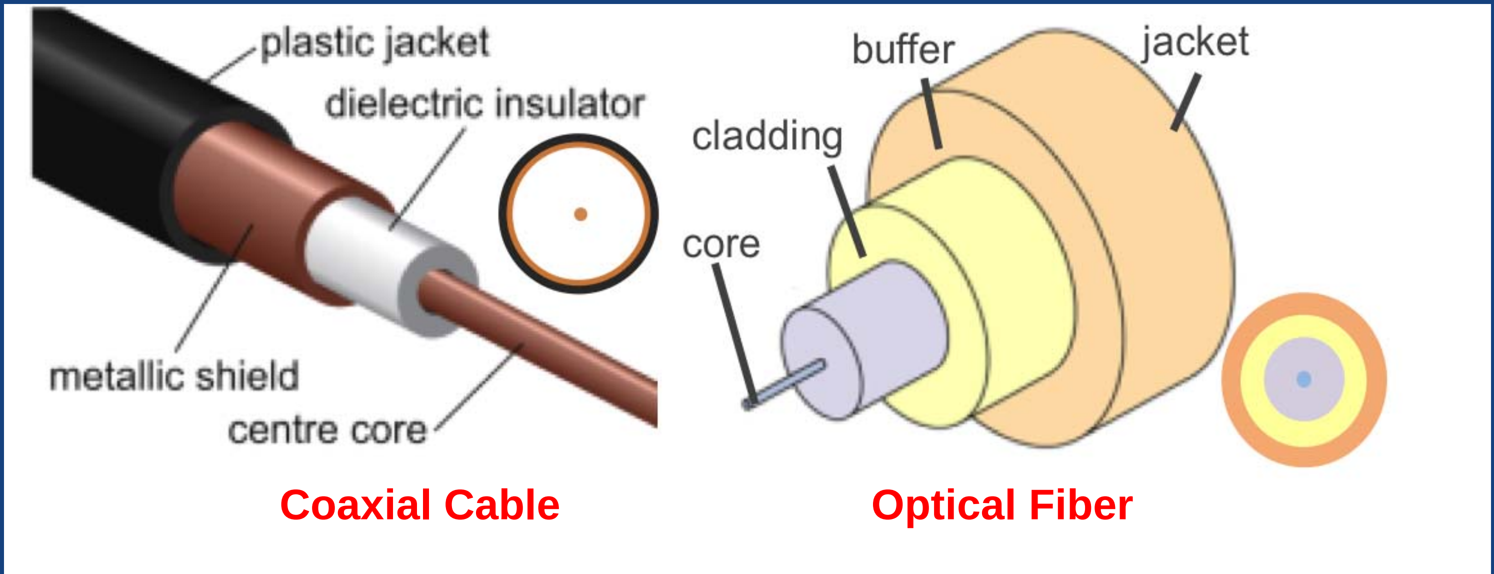

4.1 Fiber Optic Interferometer

- Optical fiber:

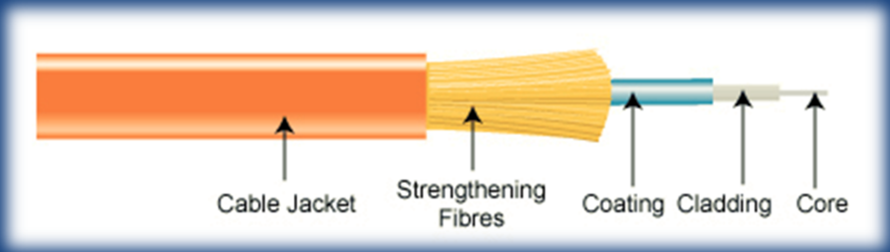

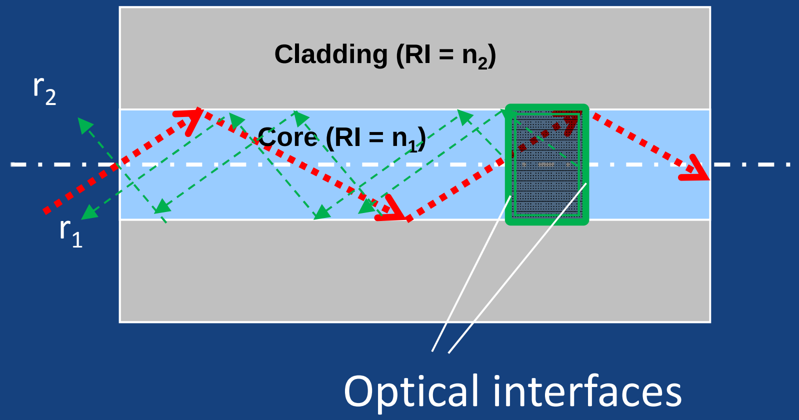

- Advantages:
  - High resolution, fast response
  - Small size
  - Potential for multiplexing and distributed measurement
- Major issues:
  - Thermal stability
  - Mechanically weak/fragile
  - Challenges in protection and packaging

4.2 Coaxial Cable Fabry-Perot Interferometric (CC-FPI) Sensor

- **Principle of the CC-FPI sensor operation**
  - **Device:** RF interferometer analog to fiber optic interferometer
  - **Mechanism:** interference generated by reflectance from reflectors (ε disturbance)
  - **Detection:** Shift of interferogram

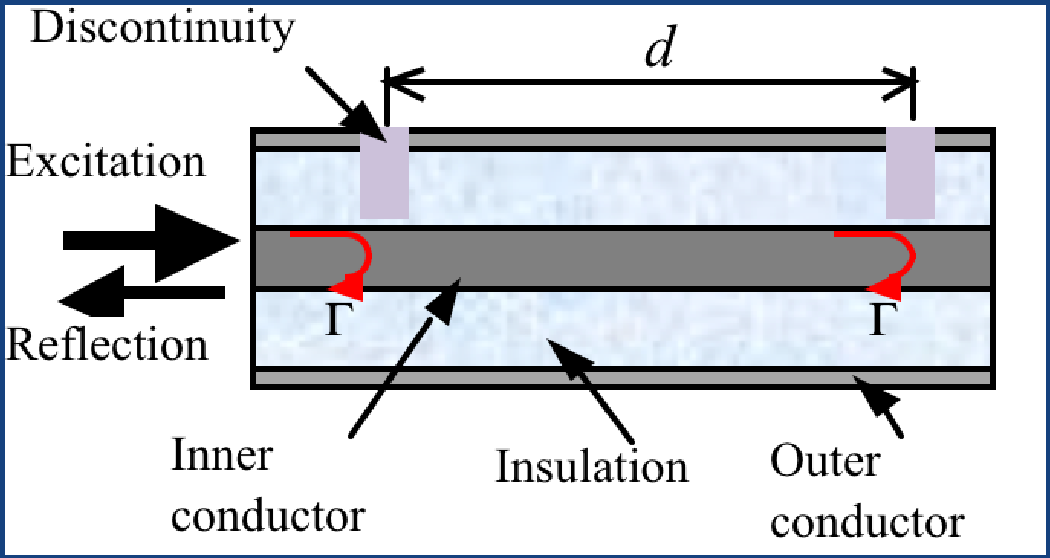

4.2 CC-FPI Temperature Sensing Mechanism

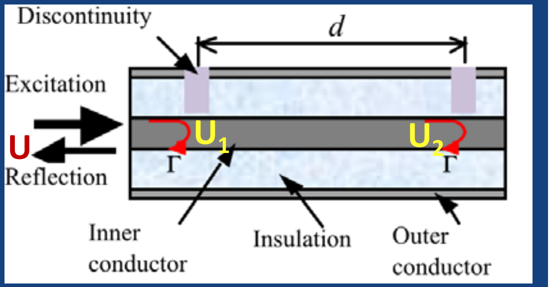

- Two reflected waves (*U1* and *U2*)

$$U_1 = \Gamma(f)e^{-\alpha z}\cos(2\pi ft) \quad \text{and} \quad U_2 = \Gamma(f)e^{-\alpha z}\cos\left[2\pi f(t+\tau)\right]$$

$$\textit{where} \quad \tau = 2d\sqrt{\varepsilon_r}/c$$

- Interference signal (U) – summation of the two reflected waves

$$U = 2\cdot\Gamma(f)e^{-\alpha z}\cos\left(2\pi f\frac{2d\sqrt{\varepsilon_r}}{c}\right)\cos\left[2\pi f\left(t+\frac{2d\sqrt{\varepsilon_r}}{c}\right)\right]$$

- CC-FPI Structural parameter (d) and (insulator) material property (ε_r) are temperature dependent

$$d_T = d_0 + d_0\beta_T(T\text{-}T_0)$$

- U(T) is thus a function of temperature *- real-time temperature measurement by monitoring the interferometric spectrum shift, U(T)*

$$U(T) = K_1\cos(K_2\cdot\tau(T))\cdot\cos[K_2(t+\tau(T))]$$

$$\tau(T) = 2d_T\cdot\varepsilon_{r,T}^{0.5}/c$$

4.3 Multiple CC-FPI Sensors for Distributed Temperature Measurement

- Distributed CC-FPI sensor
  - multiple FPI along a single coaxial cable
- Weak reflections and low insertion loss
  - enable long distance coverage
- Individual sensor location
  - *achieved by a novel joint time-frequency domain measurement technique (Xiao et al., 2013/CU)*
- Reflected EM waves detected by a VNA resolving:
  - Amplitude
  - Phase

- *Goal:*
  - *Resolution/*accuracy: ±2°C
  - measuring a range: 350 – 1000°C
  - spatial resolution: <10 cm

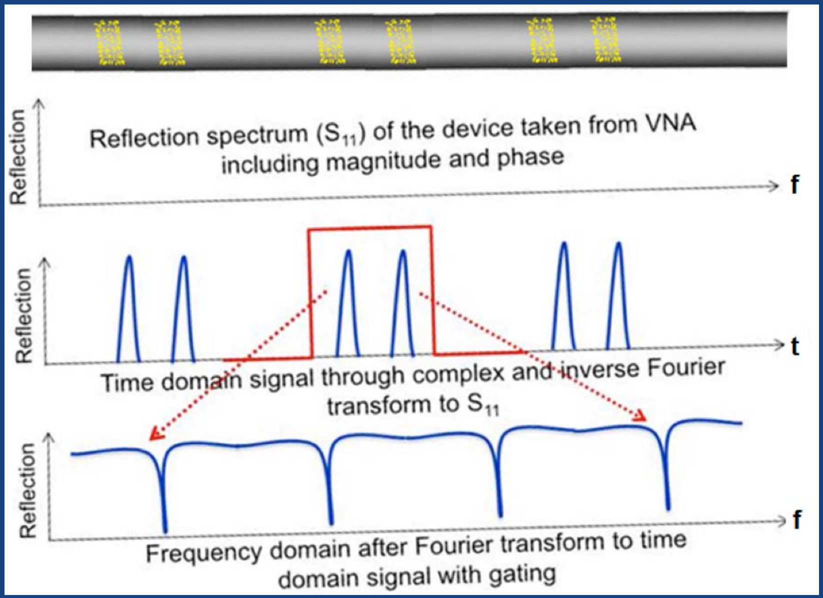

Joint-time-frequency domain interrogation of multi-point FPI in a single cable for distributed sensing with high spatial resolution

4.4 Key Issues To Be Addressed for Realization of the MCCC-FPI Sensors

1. Commercial CC are ***NOT*** for high temperature applications - **MCCC materials for the proposed high-temperature FPI sensors are currently nonexistent.**
2. Limited metal-ceramic CC are for high temperature RF communication are ***NOT*** suitable for MCCC-FPI construction
3. Current fabrication method and FPI structures are ***NOT*** suitable for in-situ applications in fossil energy system
4. Structural parameters (i.e. element dimensions) and insulator/reflector ε_r-contrast need to be optimized
5. Structural and material stability in harsh conditions and impact on sensor performance must be understood

4.4 For High Temperature Monitoring:
MCCC-FPI (MCCC-FPI) Distributed Sensors

- Metal conductors (tube and wire) with ceramic (or air) insulation (or reflectors)
  - Metal tube may eliminate bulky and expensive protective packaging
  - Withstand highly turbulent and erosive flows
  - Minimize destruction to the equipment for installation and maintenance

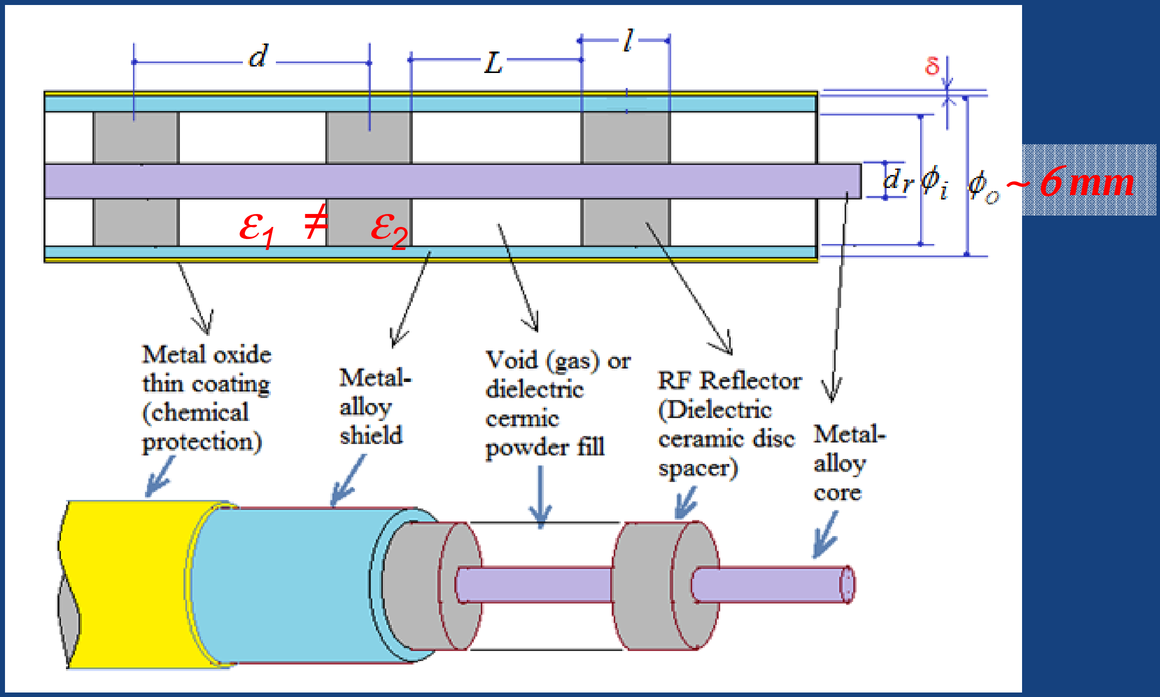

4.6 Research Focuses

1. *Developing MCCC Materials*
2. *Fabricating MCCC-FPI Sensors*
3. *Demonstrating Temperature Measurements up to 1000^{o}C*

4.7 MCCC-FPI Test Apparatus

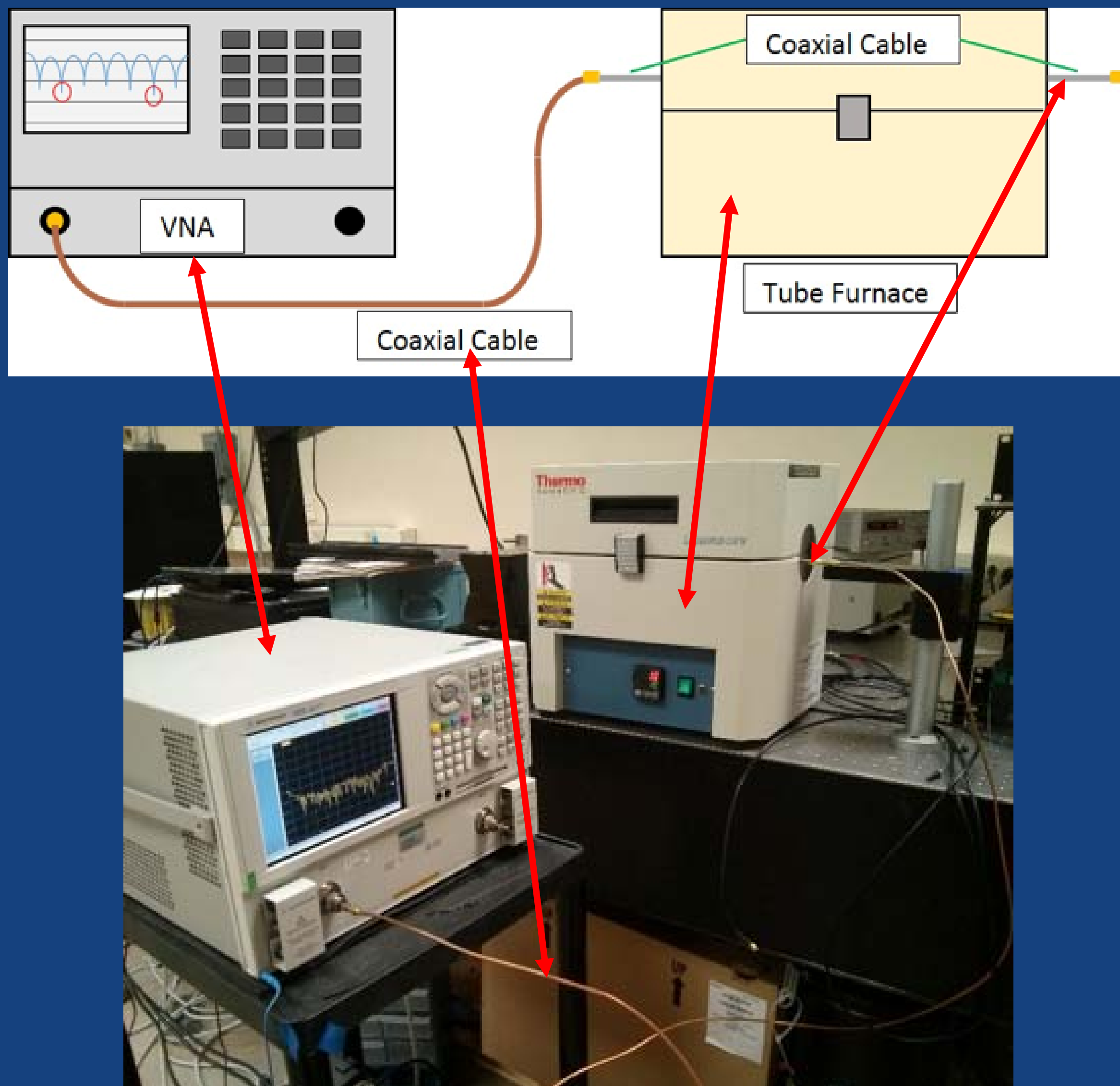

5. MCCC-FPI Sensor Fabrication and Test

5.1 Ceramic Tube Insulator with Circular Air-Gap Reflectors

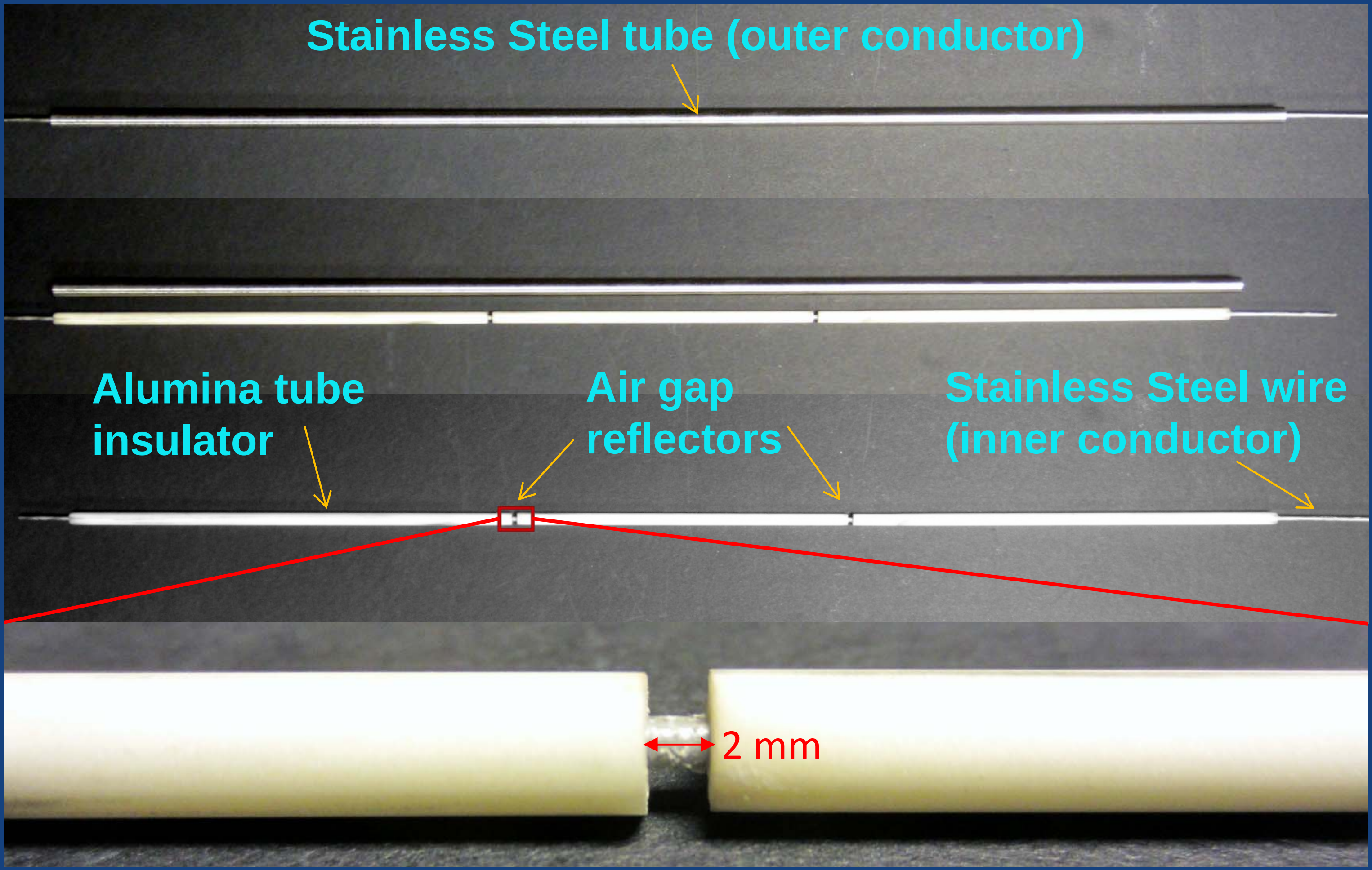

5.1 Temperature Measurement Test

- **Single point CC-FPI:** stainless steel conductors (tube and wire), alumina insulator, and air gap (~1 mm) reflectors.
- Strong "*Δf – T* " correlation (**to 900°C**) but poor consistency between cycles because of structural instability

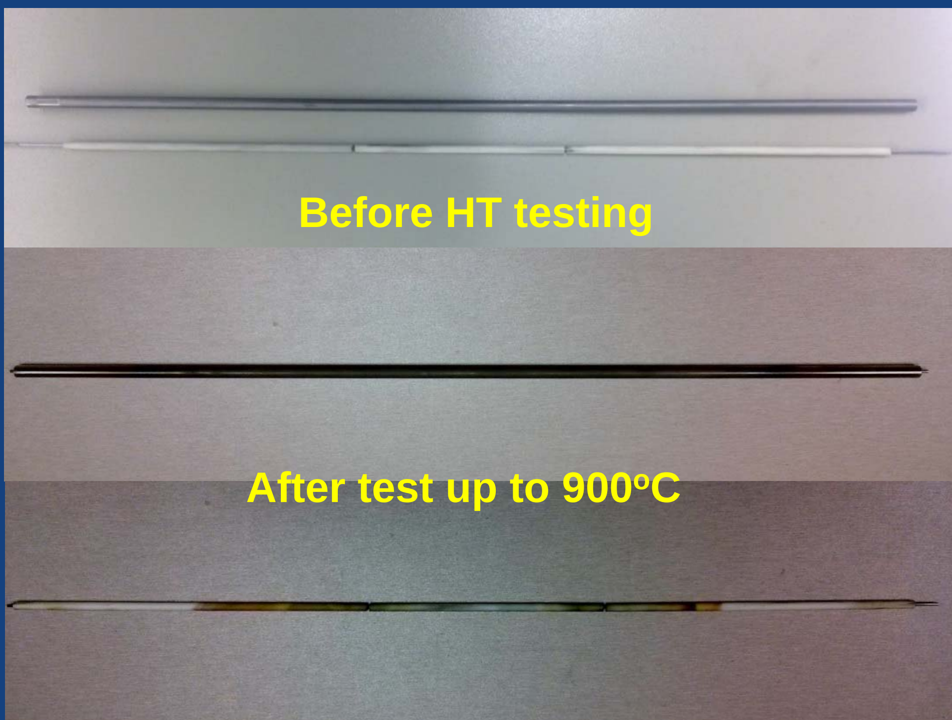

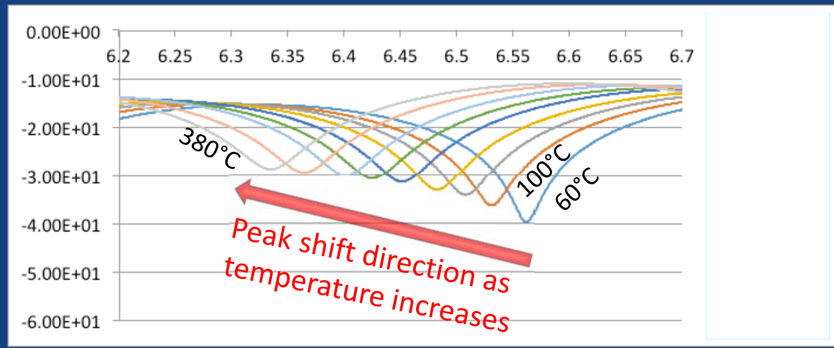

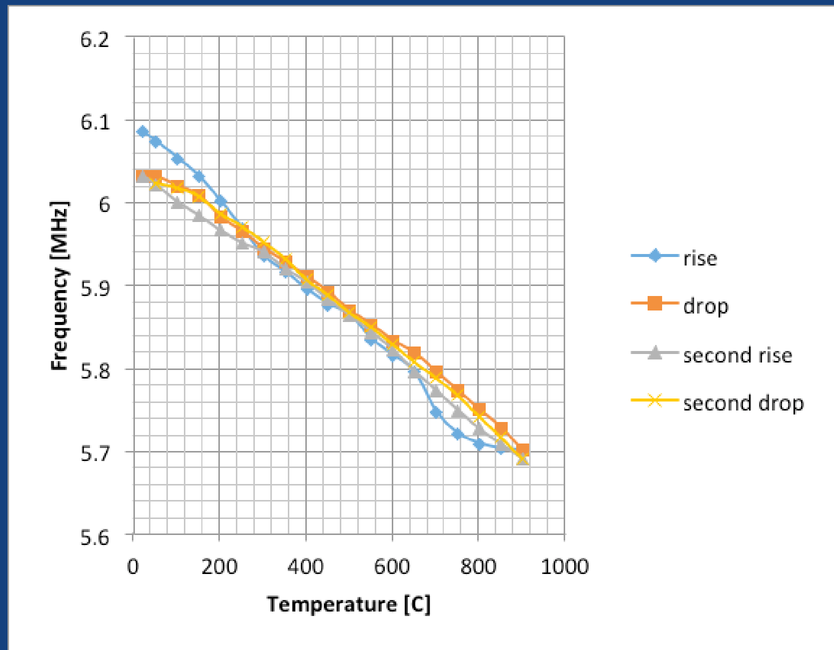

5.2 Ceramic Powder Packed-Bed as Insulator and Ceramic Discs as Reflectors (flexible)

Material	Composition	T_{max}, °C	ρ, μΩ/cm	CTE, 10^{-6} m/m·°C
Stainless steel 316	Fe with 16-18%Cr, 10-14%Ni, 2%Mo, 0.75%Si	>2000	11.6	8.9 – 11.1

Material	Composition	T_{max}, °C	ε_r, @ 1MHz	CTE, 10^{-6} m/m·°C
α-alumina	99.8% Al_2O_3	1750	9.5	8.4
Zirconia Toughened Alumina (ZTA)*	ZrO_2-Al_2O_3	1650	10.6	8.1
Sapphire (SAP)*	Al_2O_3	2000	9.3-11.5	5.4
Fussed quartz (QTZ)*	SiO_2	1000	3.8	0.6
Macor® (MAC)*	SiO_2-ceramic	1000	6.03	9.4
Air	Gas (mainly N_2+O_2)	>2000	~1.0	compressible

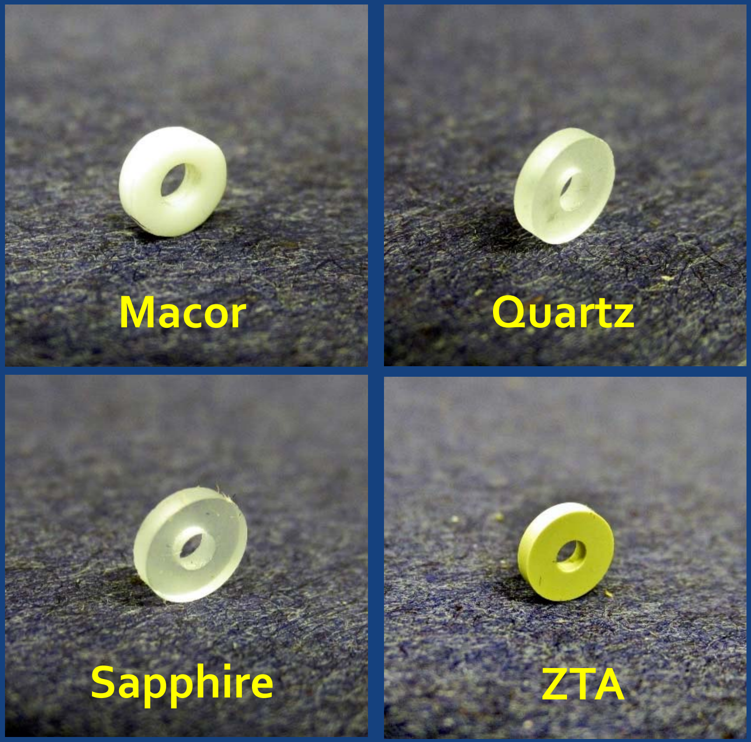

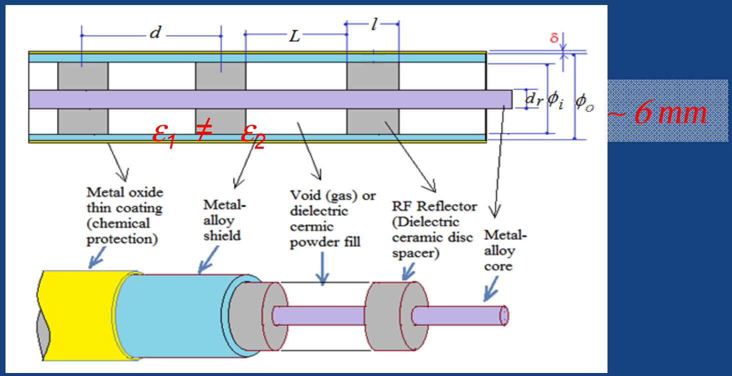

5.2 Temperature Measurement Tests

- **Single point CC-FPI:** stainless steel conductors (tube and wire), alumina tube as insulator, and ceramic discs as reflectors (thickness 1 mm).
- Good "$\Delta f \sim T$" correlation but poor consistency between cycles because of structural instability
- The measurement consistency may be improved by fixing the positions of the insulators
- More investigations will be performed if time allows since **cable flexibility could be an important advantage for practical application**

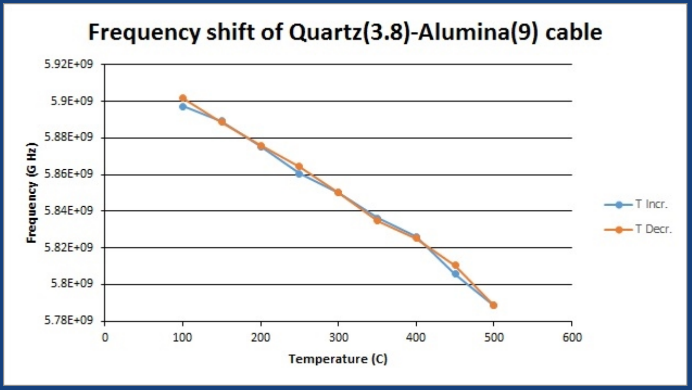

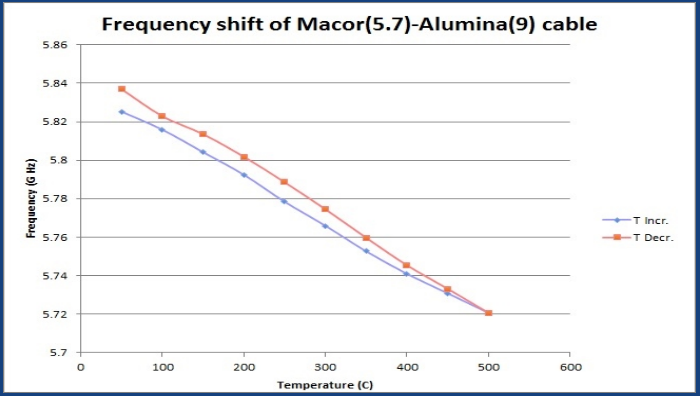

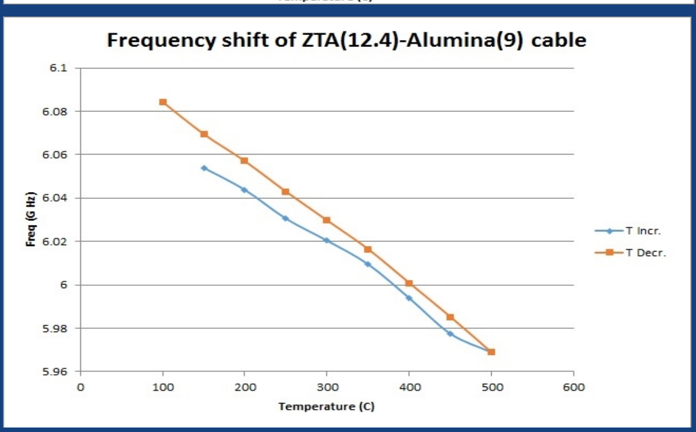

5.3 Reflectors by Casted Ceramic Discs

- **A possible way of tuning the *ε-contrast* between insulation and reflectors**
- **To fix the structure (to prevent of the insulator tubes from moving out of their positions)**
- **Temperature measurement not yet been tested**

Cast Material	Al_2O_3	SiO_2	$ZrO_2 - ZrSiO_4$
Temp. Limit (°C)	1650	1650	1760
CTE (in/in × 10^{-4} °C)	7.2	0.59	7.4
Dielectric Strength (V/mil)	171	156	188

*From AREMCO property data sheet

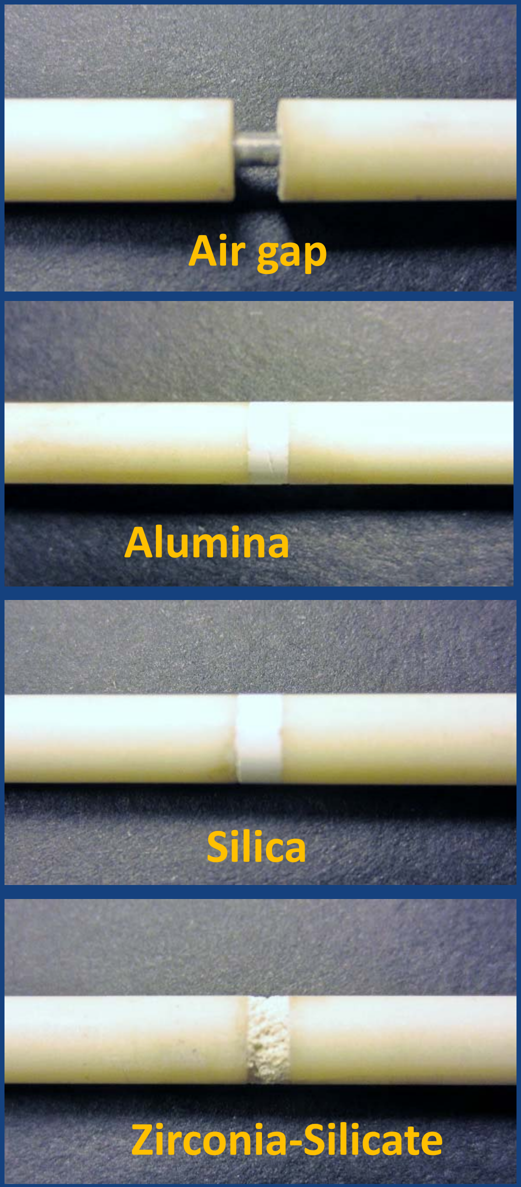

5.4 FPI Using Reflectors Created by Partial Removal of the Insulator Tube

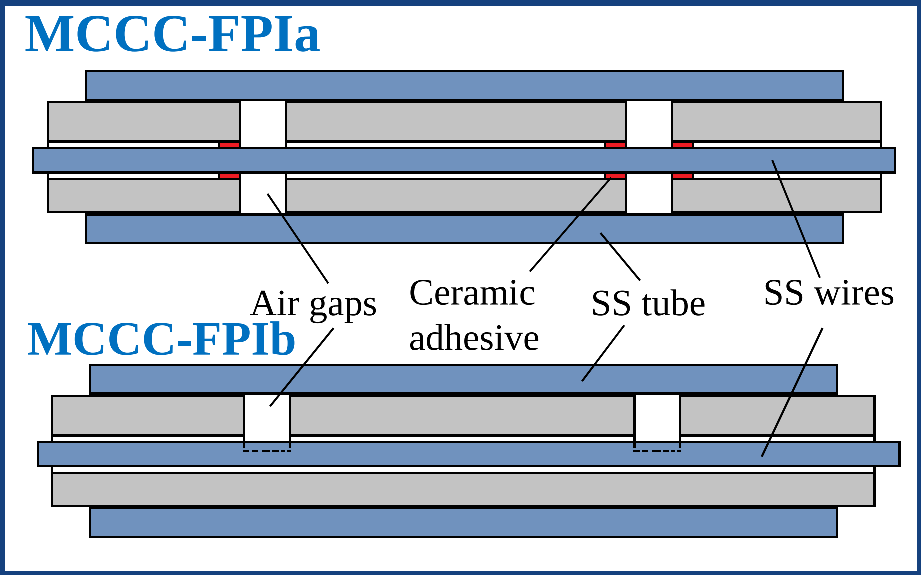

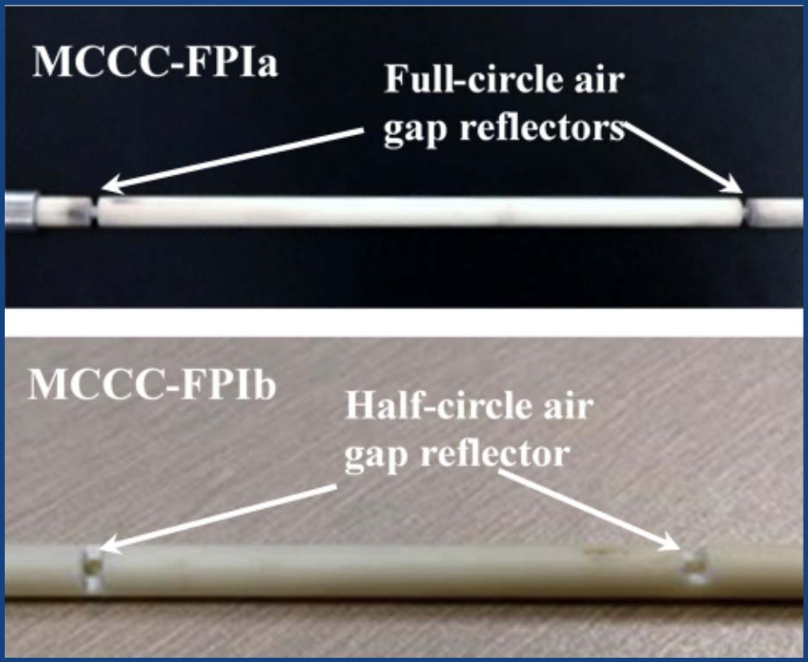

- MCCC-FPI a: **d** determined by expansion/contraction of metal wire
- MCCC-FPI b: **d** determined by expansion/contraction of alumina medium

5.4 Structure Stabilization by Thermal Cycle Pre-Treatment

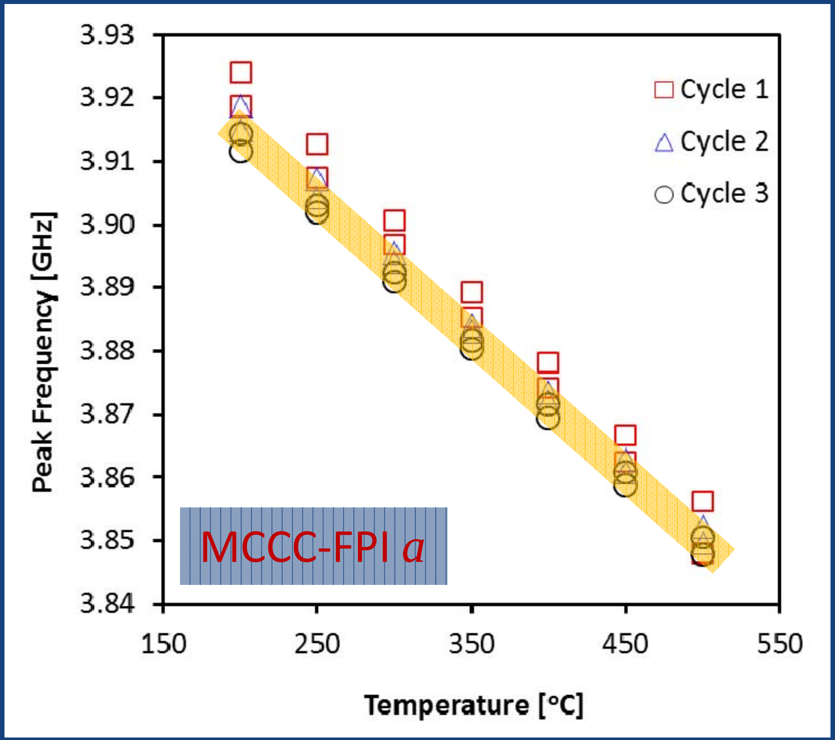

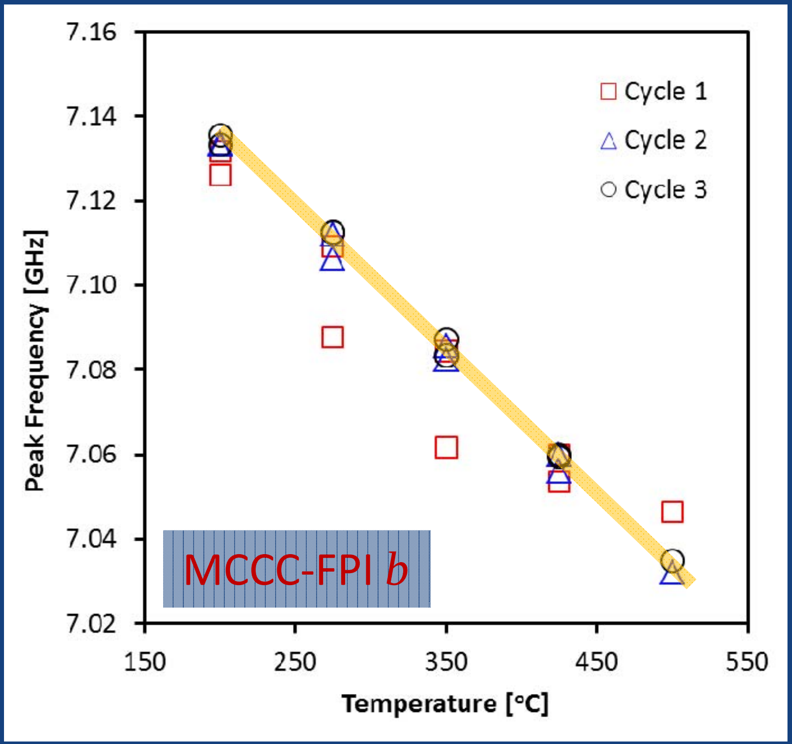

Evolution of the relationship between peak frequency and temperature during pretreatment of heating-cooling cycles

5.5 Sensor Response Speed

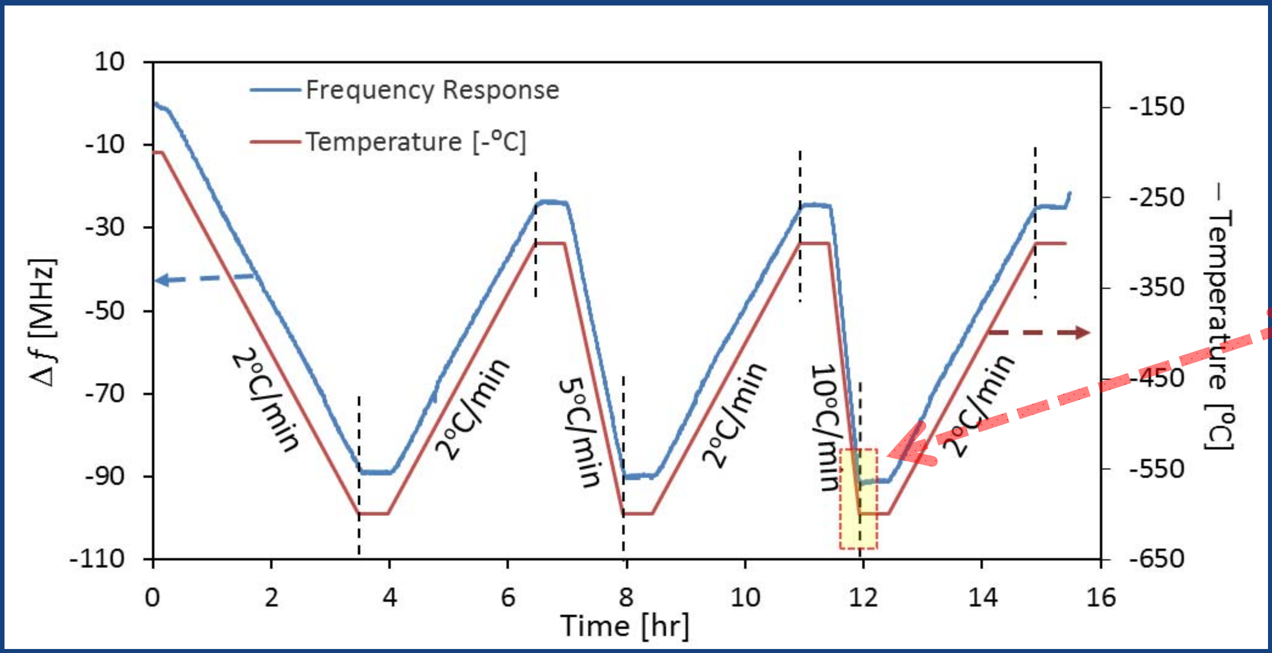

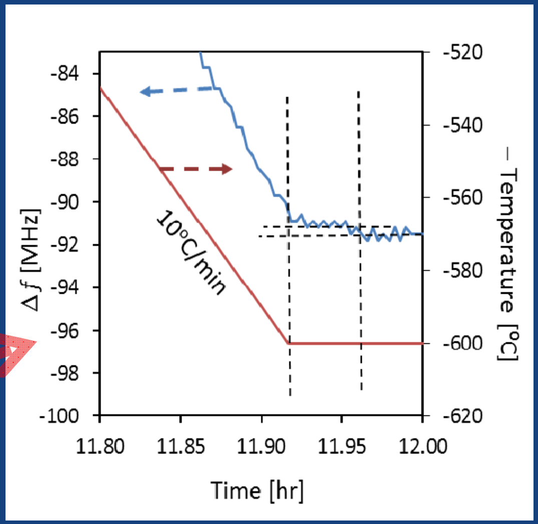

Frequency shift (Δ*f*) for MCCC-FPIa as a function of time in response to the programmed temperature change:

Response time estimated <180 seconds

5.6 Temperature-Dependence of Δ*f* and Sensitivity

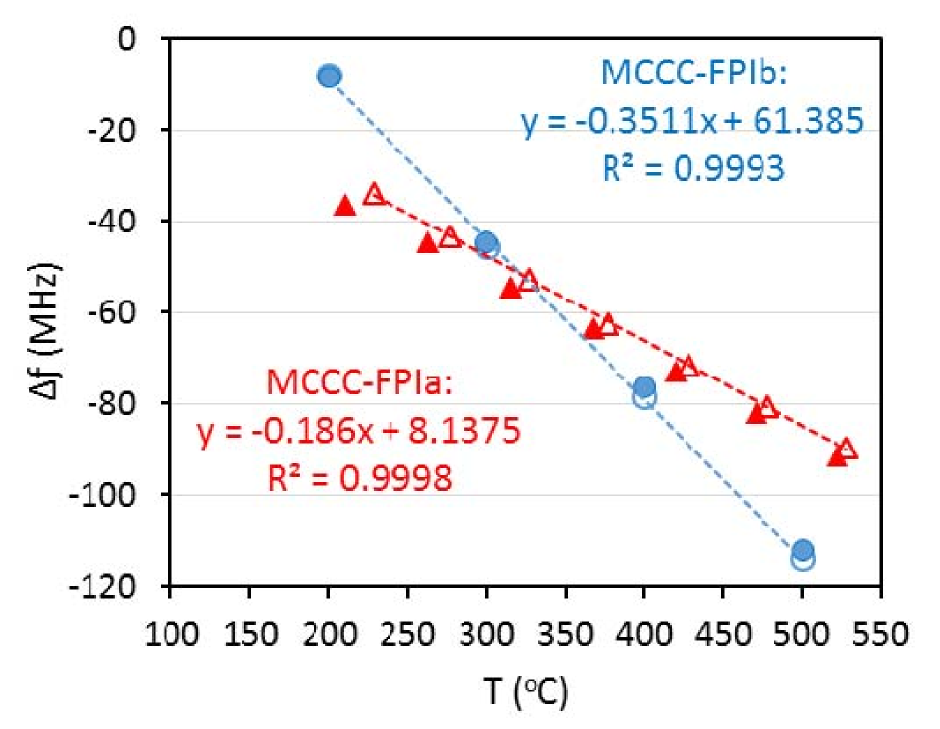

Resonant peaks used @ RT:

FPIa – 3.4 GHz; FPIb – 7.1 GHz

Temperature-dependences of Δ*f*:

Excellent linear dependence –

FPIa (-0.186 MHz/°C); FPIb (-0.351 MHz/°C)

Sensitivity:

FPIb higher than FPIa

Structure stability:

FPIb better than FPIa

Sensitivity difference caused by:

Peak *f* rather than difference in $(d_T \times \varepsilon_{r,T}^{0.5})$

Resolution (Δ*f* /°*C*): -0.35 MHz/ °*C (for FPIb)* & -0.19 MHz/ °*C (for FPIa)*

Since the VNA has a frequency scanning resolution (1 Hz) much smaller than 0.1 MHz, both sensors are in principle capable of monitoring temperature changes within ±2 °C.

5.7 Effects of Slot Width and Spacing (*d*) on Reflection Intensity

- **Reflection intensity can be adjusted effectively by varying the slot (reflector) width but almost independent of the spacing between the reflectors.**
- **These findings are useful for the design of multi-point FPI sensors.**
- **Influence of depth is being studied**

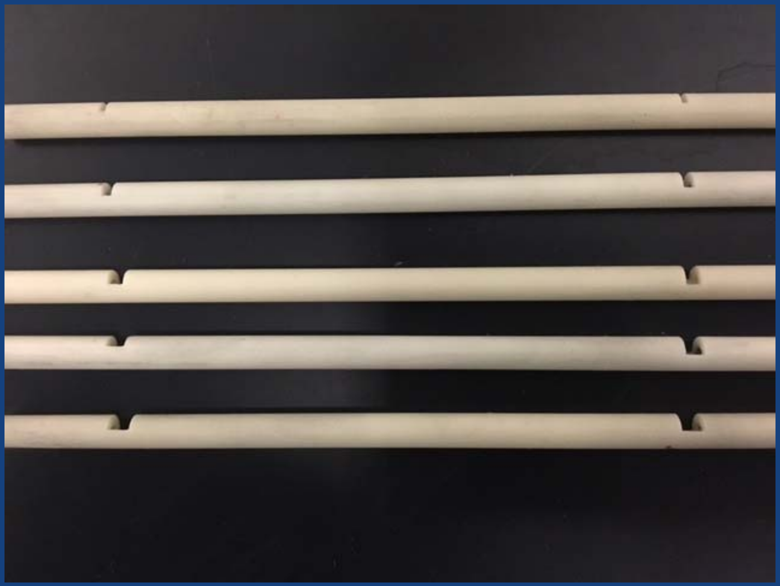

Reflector width, mm	**Relative intensities of the 1st reflector**				
Inter-reflector distance, cm	**1.0**	**1.5**	**2.0**	**2.5**	**3.0**
10.0		1.74%	1.89%	2.52%	2.59%
7.5	0.81%	1.79%	1.62%	2.01%	2.73%
5.0	0.87%	1.77%	1.82%	2.27%	2.37%

6.1 MCCC-FPI (*b*) Multi-Point Sensor

- Three-point (3 pairs of slot reflectors in line) and four-point (4 pairs of slot reflectors in line) have been fabricated (alumina tube insulator, empty slots as reflectors, and SS tube and wire as outer and inner conductors)
- The multi-point MCCC-FPI sensors have been tested for functionality of monitoring spatially distributed temperatures

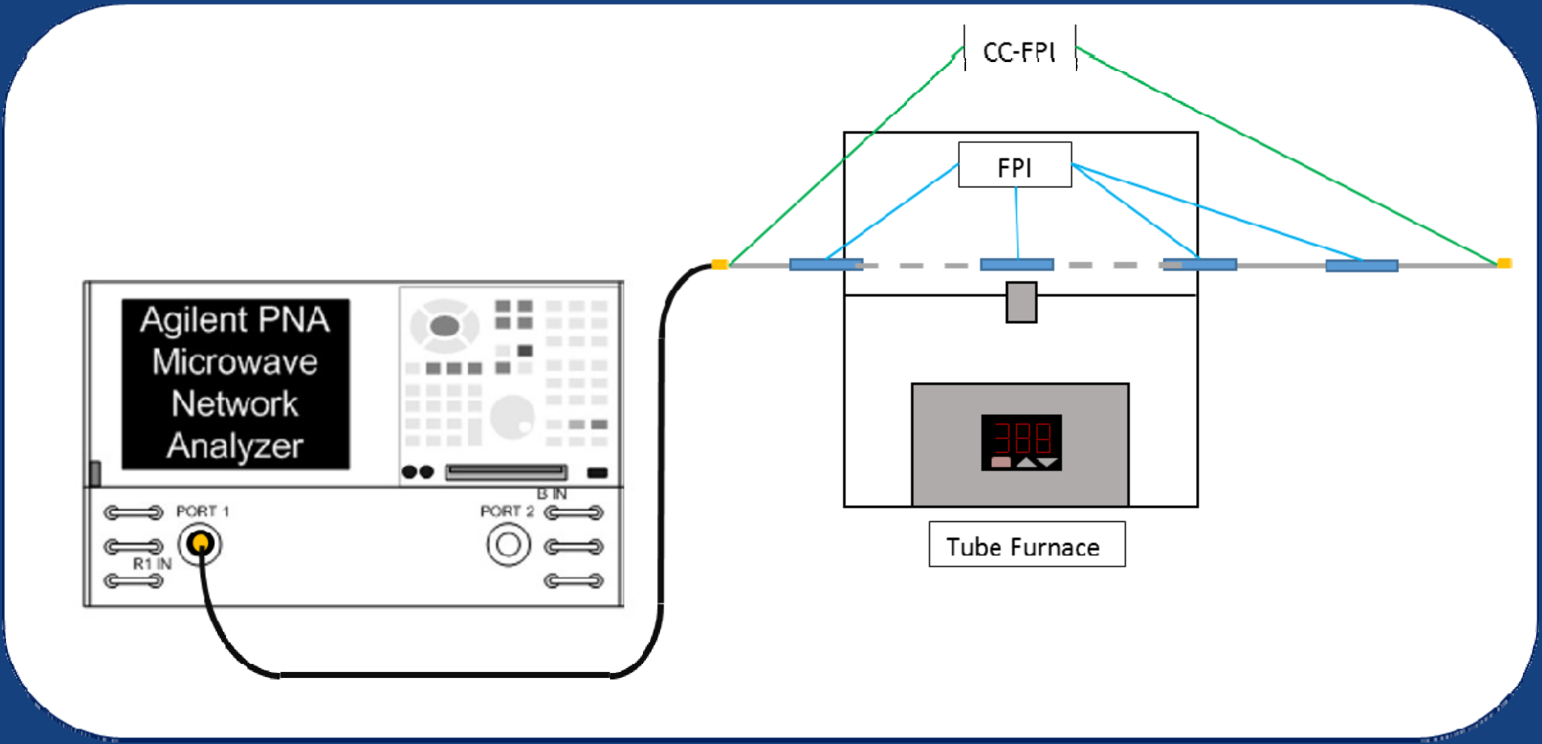

6.2 MCCC-FPI (*b*) Multi-Point Sensor Test

Three-point MCCC-FPIs

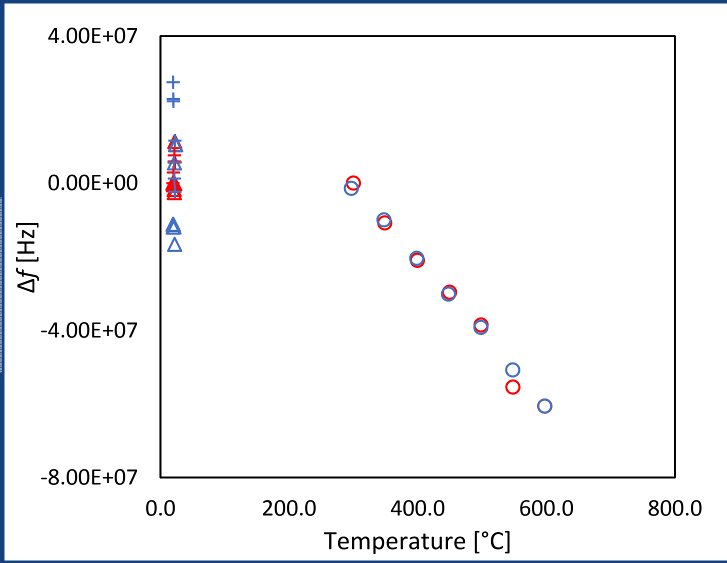

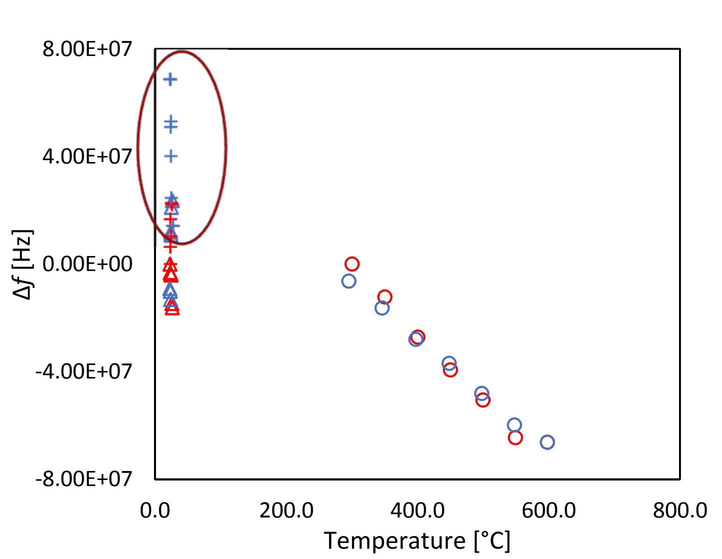

Four-point MCCC-FPIs

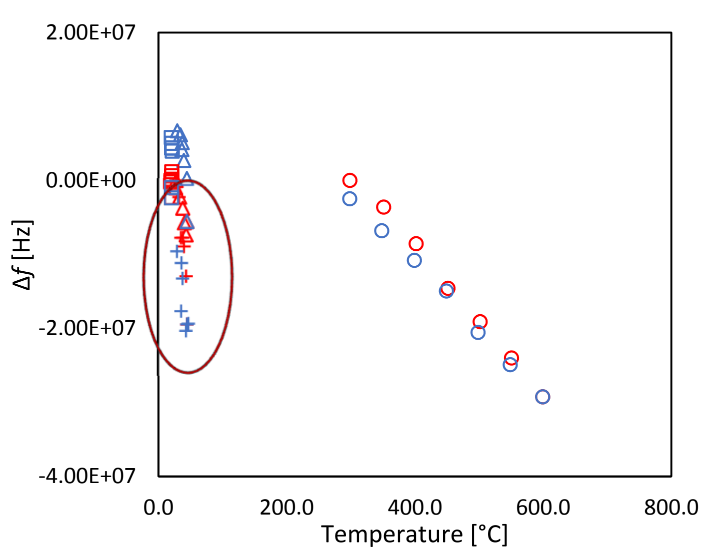

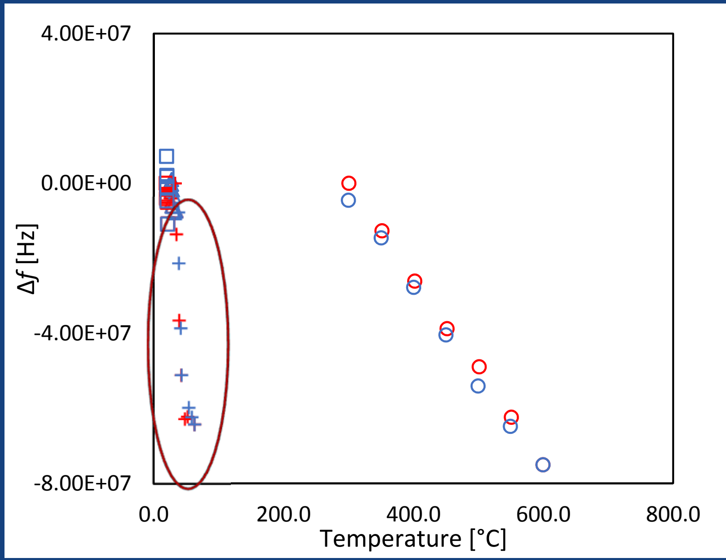

7. Cable Stability Study

- Samples of cable treated in air and in gas mixture (Air/CO/CO_2/SO_2/H_2O) at 1000°C
- SEM and EDAX characterization to examine the structural and interface chemical stability

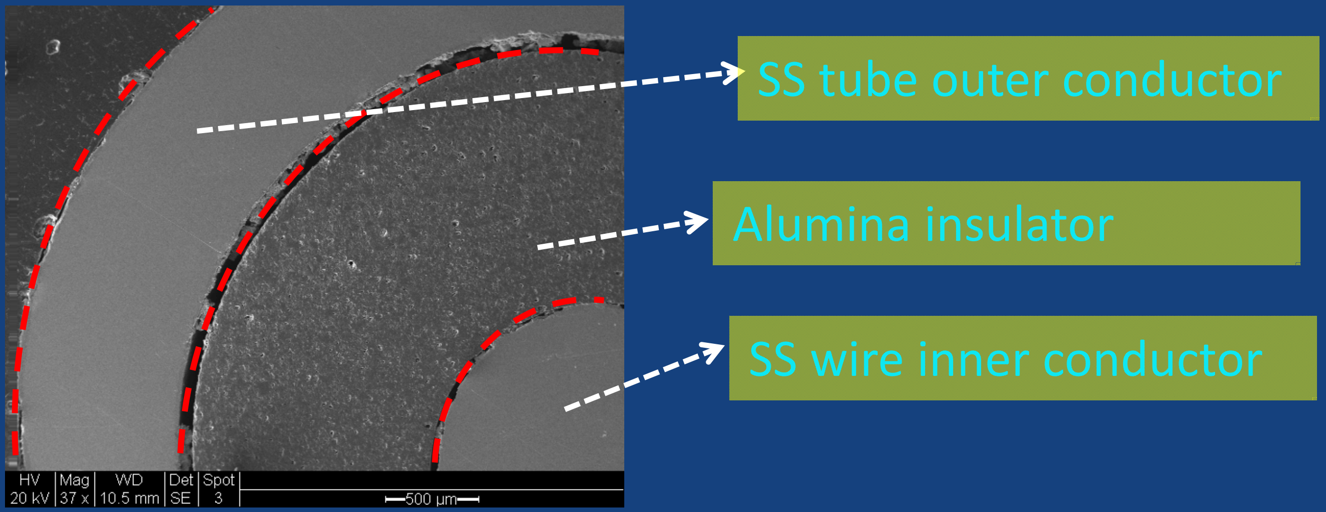

7.1 Cable Stability – alumina insulation

- Samples of MCCC subjected to HT for 168 hrs
- SEM and EDAX characterization analysis

Because the sensor elements are enclosed in metal tube, no chemical and structural damage were observed after 168 h at 1000^{o}C but stability in longer term is yet to be tested

7.2 Cable Stability – Mullite insulation

Mullite-Stainless Steel combination was also stable after 168 h at 1000°C.

8. Conclusions and Plans

1. Accomplished proof of concept for the MCCC-FPI high temperature sensor with single point FPI sensor demonstration
2. Detection resolution of >0.1 MHz/^{o}C achieved (much higher sensitivity for detecting 2^{o}C change)
3. Functionality of reporting temperature (signal) from individual FPI point demonstrated by 3-point and 4-point MCCC-FPI sensors
4. Due to the enclosure of the metal tube, the MCCC-FPI showed excellent thermal stability at 1000^{o}C for >150 h
5. **Plans:** (1) Test 3- and 4-point sensors for measurement up to 1000^{o}C; (2) Fabricate and test 1 – 2 m long multi-point MCCC-FPI sensors for measurement up to 1000^{o}C.

THANK YOU

Previous Work—Multi-Point FPI

Multi-Point CC-FPI sensor for distributed measurement

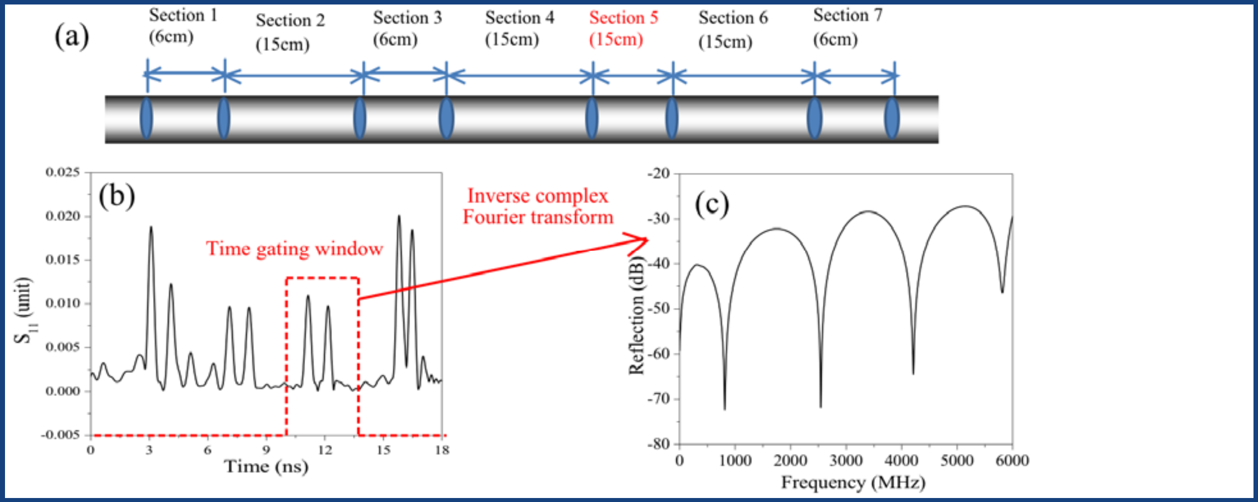

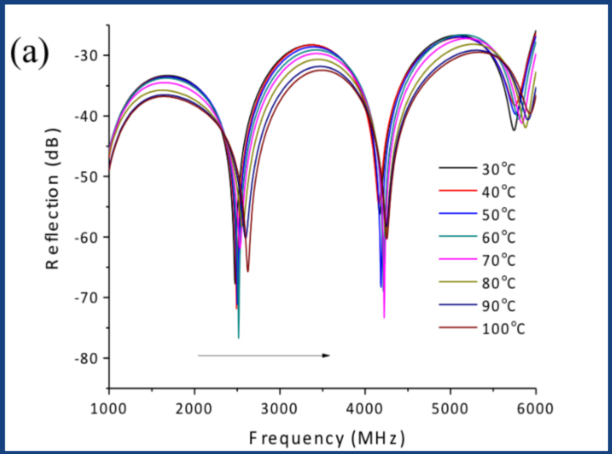

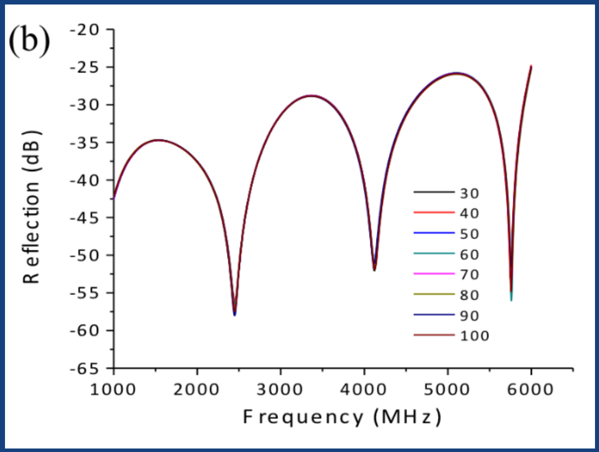

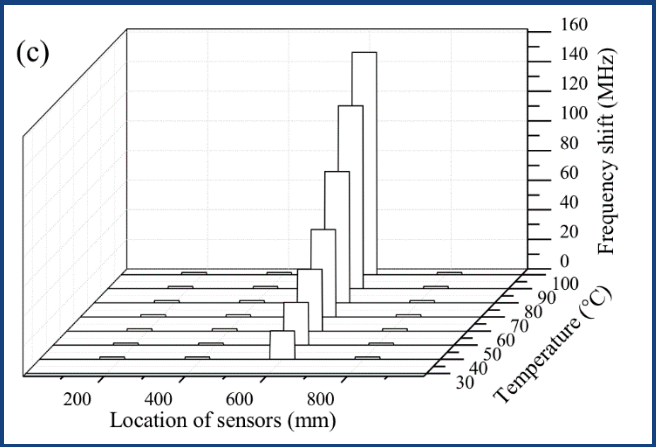

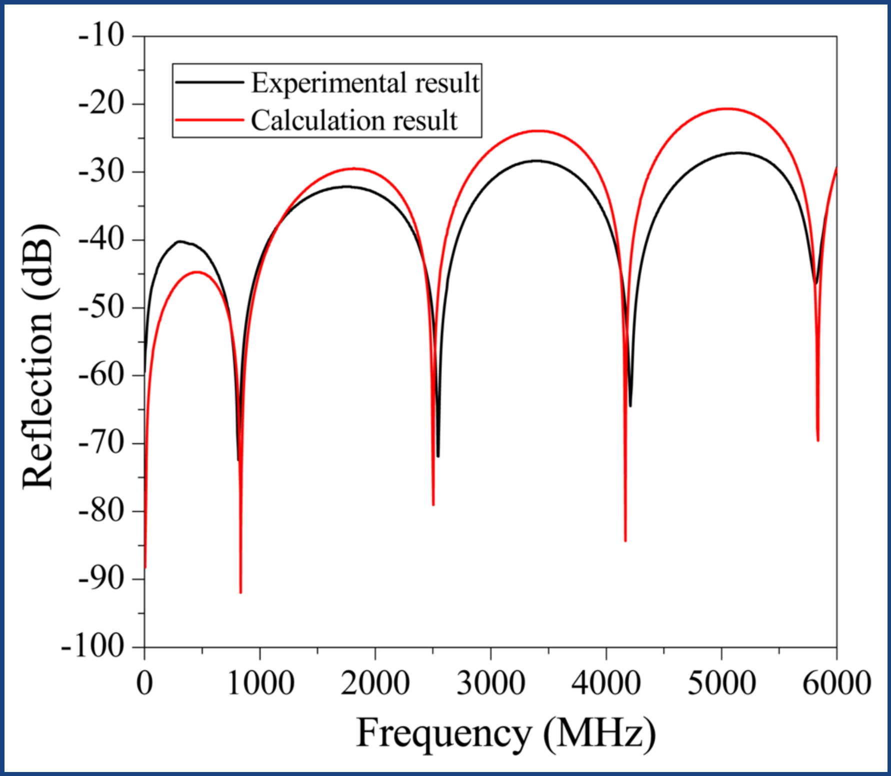
Experimental result
Calculation result
Reflection (dB)
Frequency (MHz)

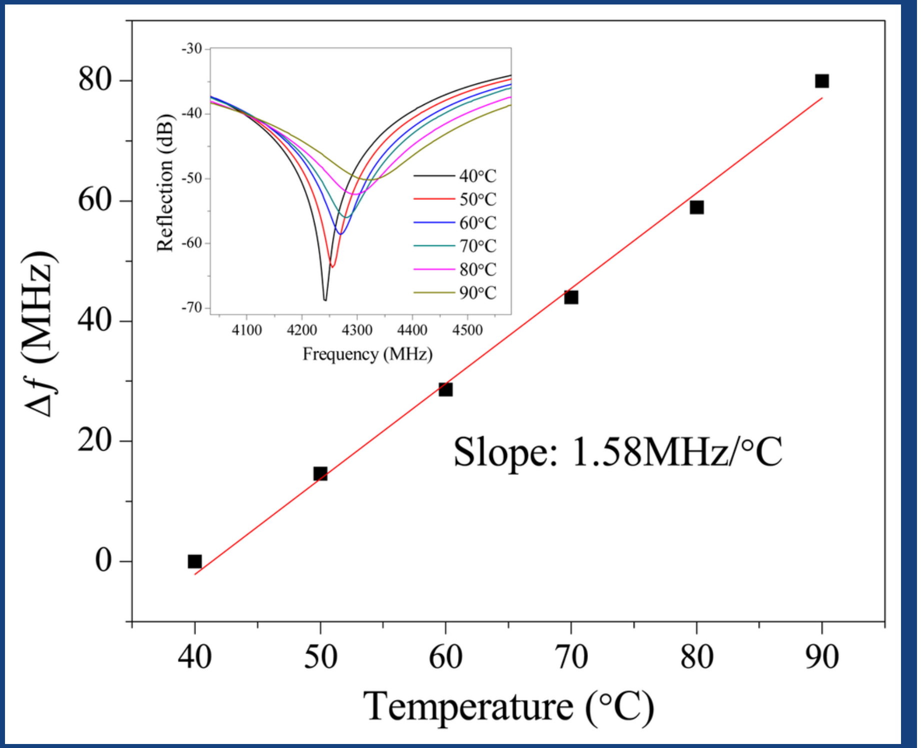
Δf (MHz)
Temperature (°C)
Slope: 1.58MHz/°C
Reflection (dB)
Frequency (MHz)
40°C
50°C
60°C
70°C
80°C
90°C

Frequency shift data

Frequency shift data in the experiments

Performance parameter	1mm MAC	1mm ZTA (Day-1)	1mm ZTA (Day-2)	1mm SAP (to 400^{o}C)	2mm QTZ
Peak frequency, GHz	5.8	6.0	6.0	6.0	5.9
Sensitivity/heating, ppm/^{o}C	40.1	40.5	40.1	80.4	46.0
Sensitivity/cooling, ppm/^{o}C	44.6	47.9	42.7	82.1	48.0
Frequency difference before after thermal cycle, MHz	11.7 (50˚C)	15.6 (150˚C)	6.3 (100˚C)	6.3 (100˚C)	4.7 (100˚C)
Distance difference, µm	241.2 (50˚C)	312.2 (150˚C)	124.3 (100˚C)	124.3 (100˚C)	95.6 (100˚C)

The theoretical and experimental reflection intensity

	1mm MAC	1mm ZTA (Day1)	1mm ZTA (Day2)	1mm SAP (anisotropic)	2mm QTZ
Calculated reflection	10.9%	8.0%	8.0%	6.1% or 1.35%	23.2%
1st Peak 100C (exp)	1.65%	4.19%	3.99%	2.11%	5.22%
2nd Peak 100C (exp)	1.32%	3.58%	2.61%	1.81%	4.23%
1st peak 500C (exp)	3.50%	2.84%	2.43%	0.66%	6.07%
2nd peak 500C (exp)	2.66%	2.69%	2.72%	0.49%	5.70%
1st peak Intensity with rising temp.	Increasing	Decreasing	Decreasing	Decreasing	Increasing

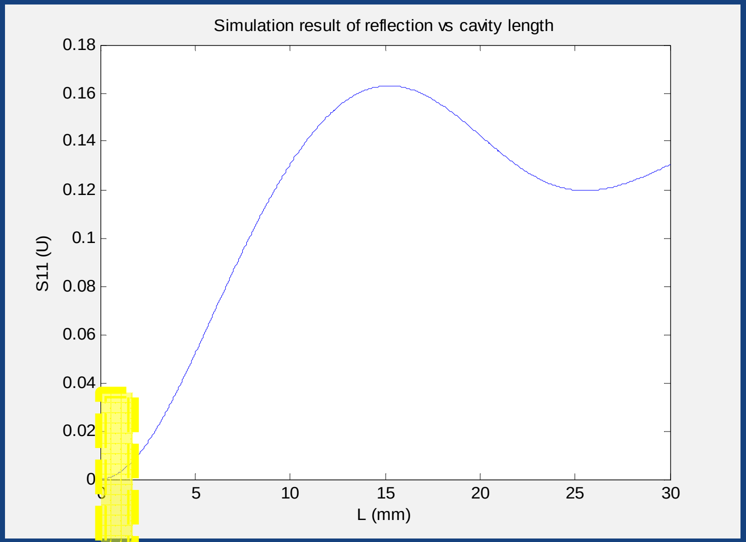
Simulation result of reflection vs cavity length
S11 (U)
L (mm)

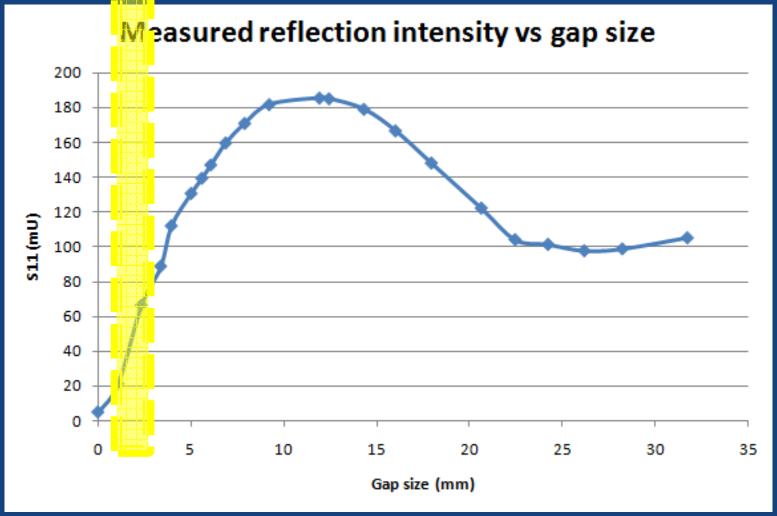
Measured reflection intensity vs gap size
S11 (mU)
Gap size (mm)

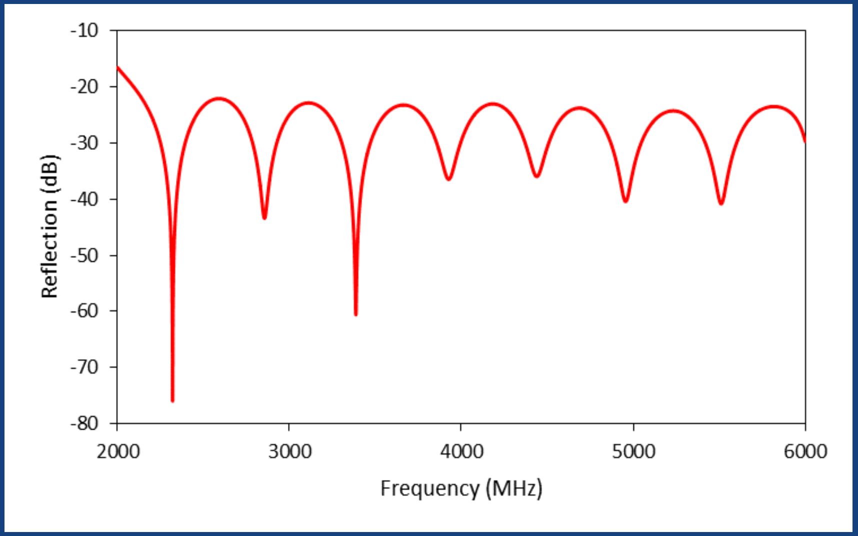
Reflection (dB)
Frequency (MHz)